Proceedings of the 11th International Symposium on Unmanned Untethered Submersible Technology, 1999, Pp. 415-426.

A MECHANICAL MODEL FOR THE RAPID BODY FLEXURES OF FAST-STARTING FISH

Peter J. Czuwala[+], Craig Blanchette[+], Stephanie Varga[+],
Robert G. Root[++], and John H. Long, Jr.[+]

[+] Department of Biology, Vassar College, Poughkeepsie, NY, 12603
(914) 437-7276 voice, (914) 437-7315 fax,
peczuwala@vassar.edu, crblanchette@vassar.edu, jolong@vassar.edu
[++] Department of Mathematics and Computer Sciences, Lafayette College, Easton, PA, 18042,
(610) 250-5280 voice, robroot@cs.lafayette.edu

Abstract

To understand the mechanical behavior of fast-starting fish, we modeled the pumpkinseed sunfish, *Lepomis gibbosus*, as a longitudinally-loaded beam that behaves as an elastic column eccentrically-loaded by lateral musculature. Since bending moments are a function of the shape of the body, we used real sunfish to determine, (1) from cross-sections, the effective moment arm of the lateral musculature, and, (2) from high speed video, the points about which the body bends. Since electromyography of fast-starting fish revealed simultaneous activation of both sides of the lateral musculature in stage 1 of a C-type start, we used this pattern to model the internal forces from which the reactive loads were determined. The model predicts that fast-starting sunfish produce a standing wave of bending moment posteriorly that then becomes a traveling wave of bending moment moving caudally from the anterior region. At the time of the standing moment wave, the body reaches its maximal effective flexural stiffness and, as a result, would be able to rapidly transmit bending moments along the body axis.

Introduction

Fish achieve peak swimming performance, in terms of acceleration of the body's center of mass, by generating high-amplitude deflections of the body, from rest or while steadily swimming, a behavior known as a fast start (Jayne & Lauder, 1993; Domenici & Batty, 1994; Domenici & Blake, 1997). Fast starts occur rapidly, with maximal reconfigurations of the body occurring within 30 to 50 ms of the initiation of bending (Westneat et al. 1998). This initial body bending, marked by the whole-body C-shape of stage 1 of the fast start, is a preparatory phase that places the median fins in a position to generate translational thrust during stage 2, the propulsive phase during which fish's center of mass accelerates maximally. Our goal is to understand how, during stage 1, muscle forces are converted to bending moments and lateral deflections along the body; in so doing, we seek to understand the mechanical design principles that permit peak swimming performance.

Fast starts are activated by a task-specific Mauthner-cell neural network (Nissanov & Eaton, 1989), powered by simultaneous activation of all of the locomotor muscle segments, associated with high intramuscular pressures, and using elastic energy mechanisms (Westneat et al. 1998). Behaviorally, fast starts are an important predator-avoidance response (Beamish, 1978; Webb & Blake, 1985; Harper & Blake, 1990), with the actual response time a function of fish size and turning angle (Domenici & Blake, 1991, 1993; Domenici & Batty, 1994). Fast starts have been investigated biomechanically (Weihs, 1973; Webb, 1976, 1977, 1978; Harper & Blake, 1990; Domenici & Blake, 1991, 1993; Westneat et al., 1998), physiologically (Eaton et al., 1977, Nissanov & Eaton, 1989; Covell et al., 1991, Beddow et al., 1995, Johnson et al., 1993, 1998), and as a measure of propulsive performance (Frithe and Blake, 1991, 1995; Gamprel et al., 1991; Kasapi et al., 1993). Weihs (1973) was the first to kinematically classify an L-type (now referred to as the C-type) fast start as consisting of three stages: stage 1, the preparatory stroke; stage 2, the propulsive stroke; and stage 3, the swimming or coasting stage. The onset of stage 1 is

characterized by electromyographic (EMG) activity patterns of synchronous onset along the length of the fish; EMG offset, however, propagates posteriorly with an increase in duration from 11 to 15 ms (Eaton et al., 1981; Jayne & Lauder, 1993). The time delay between Mauthner cell firing and the first EMG signal is approximately 2 ms while the delay between EMG signal and movement is about 6 ms. The actual demarcation between the onset of stage 2 and the offset of stage 1 has been defined according to kinematic and electromyographic parameters such as a return tail flip and contralateral EMG activity, respectively (Jayne & Lauder, 1993).

Various models have been proposed to describe the internal dynamics of steadily-swimming fish (Hess & Videler, 1984; Cheng & Blickhan, 1994; Cheng et al., 1998). Hess and Videler's model (1984) assumed that fish swim with only small amplitudes of lateral body deflection and without axial periodic motion. Cheng et al. (1998) and Cheng and Blickhan (1994) also assumed small lateral deflections, as required by the elastic curve equation; in addition, their models assumed a constant flexural rigidity along the length of the fish. We needed to relax these assumptions in order to model the bending mechanics of stage 1 of C-type fast starts, which have large amplitudes of lateral body deflection and muscularly-driven changes in flexural rigidity (Westneat et al. 1998). To this end, we propose a simple analytical model — what we call a beam-column — whereby the body of pumpkinseed sunfish undergoing a stage 1 C-start is a central, non-rotating elastic column continuous with, at both ends, a rotating beam.

Beam-Column Model

As a pumpkinseed sunfish, *Lepomis gibbosus*, performs stage 1 of a C-type fast start, its body rotates and bends laterally (Fig. 1). However, it appears that rotation occurs only in the rostral and caudal regions while the mid-body undergoes deflection; *i.e.,* the whole fish does not undergo rotation during stage 1. Since lateral body deflection and locomotion associated with C-starts usually occur in two-dimensions (Webb, 1978; Domenici and Blake, 1997), we present a two-dimensional (2-D) analysis.

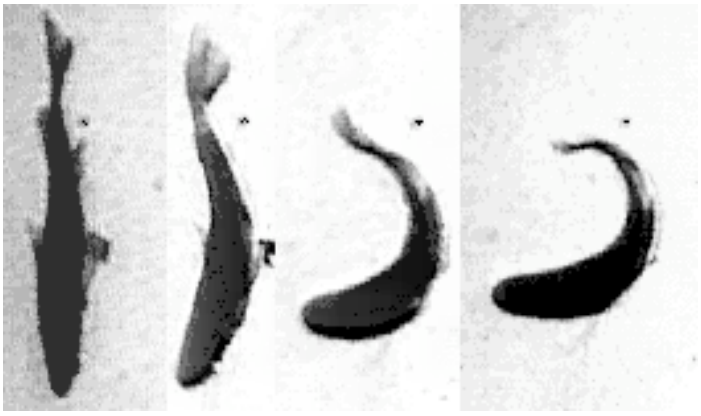

Figure 1. Fast-starting pumpkinseed sunfish, *Lepomis gibbosus* (14 cm total length). Stage 1 of a M-cell-initiated C-type start, as seen in high speed video images, from left to right at time 0, 10, 20, and 35 ms. Please note that electrical activity patterns (see Fig. 4) indicate simultaneous activation of the lateral muscles from head to tail and on both sides. The black point in each image is the fixed spatial reference.

We define our local coordinate system as originating at the head, where the positive x-axis is directed along the initially straight midline of the fish (rostral to caudal), the positive y-axis is directed laterally, and the positive z-axis is directed ventral-to-dorsal (out of the page) so as to form a right-handed coordinate system (Fig. 2). Since a typical fast-start is characterized by simultaneous contraction of the contralateral musculature (Westneat et al. 1998), it is reasonable to assume that the axial skeleton is loaded in compression. In addition, these internal muscular forces produce external reactive loads which are imposed upon the fluid. For our initial model, we represent these external reactive forces, R, W and T, as point loads which act at the head, point of maximal lateral deflection, and caudal fin, respectively. Since fast-start motion appears to consist of linear and angular (rotational) accelerations of the rostral and caudal fin regions, with simultaneous deflection of the mid-body region (see Fig. 1), we define two

transition points (TP) which delineate the axial length and placement of column-like lateral deflection within the entire fish. The external reactive loads of R, W and T are solved in terms of the muscular forces which initiate motion by applying the method of sections (Hibbeler, 1978; Beer & Johnston, 1977) independently to the various sections.

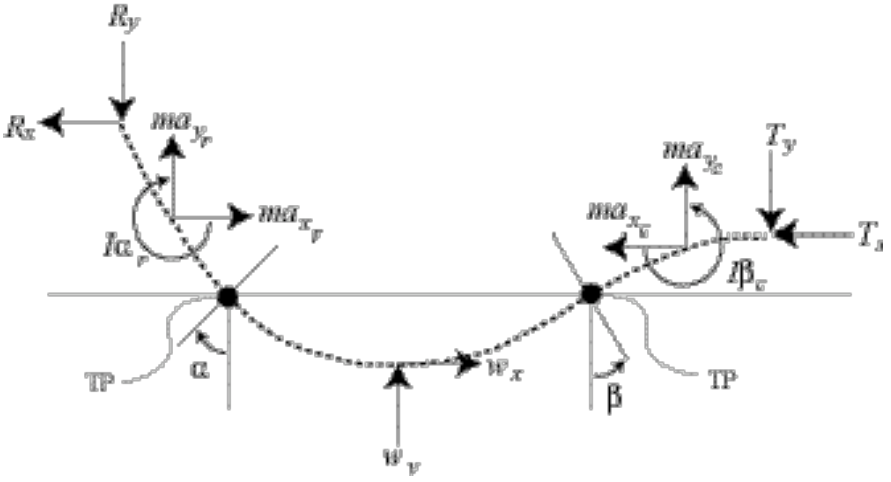

Figure 2. The fast-starting sunfish, modeled in a free-body diagram. The midline of the fish (curved, dashed line) is composed of a central column, defined as the section between transition points (black circles labeled TP) from column to rostral and caudal beams, whose bending is caused by moments produced by eccentric axial muscle force. See text for explanation of forces and moments.

Force and Moment Equilibrium — Method of Sections

Within our local coordinate system, we define the two transition points (TP) of the mid-body region as being located a distance $r = r_R$ and $r = r_C$ from the snout tip such that forces acting upon the region of the fish in-between the TP cause lateral deflection, while the forces acting rostral and caudal to the TP cause linear and rotational acceleration. Hence, for the rostral region,

$$\sum F_X : \quad [-A_{RX} + F_{IX} + F_{CX} - R_X] (i) = [m_R a_X] (i) \tag{1}$$

$$\sum F_Y : \quad [F_{IY} - F_{CY} + A_{RY} - R_Y] (j) = [m_R a_Y] (j) \tag{2}$$

$$\sum M_Z : \quad [(r_{PR} \times R) + (r_I \times F_I) + (r_C \times F_C) + (r_A \times A_R)] (k)$$
$$= [(r_{PG} \times m_R a) + I_{RZ} \alpha_{RZ}] (k), \tag{3}$$

where A_R is the resultant reactive force vector acting upon the axial skeleton are $r = r_R$, and A_{RX} and A_{RY} are the resolved forces of A_R acting parallel to the x- and y-axes, respectively; F_I is the resultant muscle force vector acting on the concave side (ipsilateral) of bending, and F_{IX} and F_{IY} are the resolved forces of F_I acting parallel to the x- and y-axes, respectively; F_C is the resultant muscle force vector acting on the convex side (contralateral) of bending, and F_{CX} and F_{CY} are the resolved forces of F_C acting parallel to the x- and y-axes, respectively; R is the resultant external reactive force vector, acting at the snout, imposed by the fluid, and R_X and R_Y are the resolved component forces of R acting parallel to the x- and y-axes, respectively; m_R is the mass of the rostral region only; a_X and a_Y are the linear accelerations parallel to the x and y-axes, respectively, acting at the mass center of the rostral region; r_{PR} is the position vector from an arbitrary midline point, P (where $0 \le P \le r_R$), to the point of application of the reactive force R; r_I , r_C , r_A are the position vectors from P to the point of application of the forces vectors F_I , F_C and A_R , respectively; and r_{PG} is the position vector from P to the mass center of the rostral portion. Further

expansion of equation 3 yields,

$$[r_{(R)Y}\, R_X] - [r_{(R)X}\, R_Y] + [r_{(I)X}\, F_{IY}] - [r_{(I)Y}\, F_{IX}] - [r_{(C)X}\, F_{CY}] - [r_{(C)Y}\, F_{CX}] + [r_{(A)RX}\, A_Y] + [r_{(A)RY}\, A_X] = [r_{(PG)X}\, (m_R\, a_Y)] - [r_{(PG)Y}\, (m_R\, a_X)] + [I_{GZ}\, \alpha_Z]. \quad (4)$$

where $r_{(R)X}$ and $r_{(R)Y}$ are the position vectors from P to the point of application of the reactive force R parallel to the x- and y-axes, respectively; $r_{(I)X}$, $r_{(I)Y}$, $r_{(C)X}$, $r_{(C)Y}$, $r_{(A)RX}$, and $r_{(A)RY}$ are the position vectors, parallel to the x- and y-axes, from P to the point of application of the force vectors F_I , F_C , and A_R , respectively; and $r_{(PG)X}$ and $r_{(PG)Y}$ are the position vectors from P to the mass center of the rostral region. Noting that a boundary condition at the snout, r = 0, is that the moment is zero; we take moments about R:

$$(\sum M_Z)_R = 0: \quad [r_{(A)RX}\, A_Y] + [r_{(A)RY}\, A_X] = -[r_{(I)X}\, F_{IY}] + [r_{(I)Y}\, F_{IX}] + [r_{(C)X}\, F_{CY}] + [r_{(C)Y}\, F_{CX}] + [r_{(PG)X}\, (m_R\, a_Y)] - [r_{(PG)Y}\, (m_R\, a_X)] + [I_{GZ}\, \alpha_Z].$$

For the mid-body region, where $r_R \le P \le r_C$:

$$\sum F_X: \quad [A_{RX} + F_{IX} + F_{CX} + B_X + P_{IX} + P_{CX} + W_X]\,(i) = [m_{MB}\, a_X]\,(i) \quad (5)$$

$$\sum F_Y: \quad [A_{RY} + F_{IY} + F_{CY} + B_Y + P_{IY} + P_{CY} + W_Y]\,(j) = [m_{MB}\, a_Y]\,(j) \quad (6)$$

$$\sum M_Z: \quad [(d_A \times A) + (d_I \times F_I) + (d_C \times F_C) + (d_B \times B) + (d_{PI} \times P_I) + (d_{PC} \times P_C) + (d_W \times W)]\,(k) = [(d_G \times m_{MB}\, a) + I_{(MB)Z}\, \alpha_{(MB)Z}]\,(k), \quad (7)$$

where B is the resultant reactive force vector acting upon the axial skeleton are $r = r_C$, and B_X and B_Y are the resolved forces of B_R acting parallel to the x- and y-axes, respectively; P_I is the resultant muscle force vector acting on the concave side (ipsilateral) of bending, and P_{IX} and P_{IY} are the resolved forces of P_I acting parallel to the x- and y-axes, respectively; P_C is the resultant muscle force vector acting on the convex side (contralateral) of bending, and P_{CX} and P_{CY} are the resolved forces of P_C acting parallel to the x- and y-axes, respectively; W is the resultant external reactive force vector imposed by the fluid, taken as acting at maximum deflection, and W_X and W_Y are the resolved component forces of W acting parallel to the x- and y-axes, respectively; m_{MB} is the mass of the mid-body region only; a_X and a_Y are the linear accelerations parallel to the x and y-axes, respectively, acting at the mass center of the mid-body region; d_A is the position vector from an arbitrary midline point, P (where $r_R \le P \le r_C$), to the point of application of the reactive force A; d_I , d_C , d_B , d_{PI} , d_{PC} , and d_W are the position vectors from P to the point of application of the forces vectors F_I , F_C , B, P_I , P_C , and W, respectively; and d_G is the position vector from P to the mass center of the mid-body region; and $I_{(MB)Z}$ and $\alpha_{(MB)Z}$ are the mass moment of inertia and angular acceleration vectors act at the mass center of the mid-body.

According to the modeling assumptions that the mid-body region only undergoes column deflection during stage 1 of the fast-start, the mid-body region, *in toto*, is not subjected to rigid body linear and angular accelerations; Therefore, $a_X = a_Y = \alpha_{(MB)Z} = 0$. Furthermore, we allow for frictionless contraction of the musculature such that the magnitude of a muscle force is transmitted throughout its length; thus, $F_I = P_I$ and $F_C = P_C$. However, since we do not assume a constant flexural rigidity along the length of the model, the actual x and y components of the ipsilateral and contralateral musculature force vectors may vary at $r = r_R$ and $r = r_C$ (Fig. 3). At $r = r_R$ the axis may rotate by some angle α while at $r = r_C$ the axis may rotate by some angle β, then,

$F_{IX} = -F_I \cos(\alpha)$, $F_{IY} = F_I \sin(\alpha)$, and $F_{CX} = -F_C \cos(\beta)$, $F_{CY} = -F_C \sin(\beta)$, and
$P_{IX} = F_I \cos(\alpha)$, $P_{IY} = F_I \sin(\alpha)$, and $P_{CX} = F_C \cos(\beta)$, $P_{CY} = -F_C \sin(\beta)$.
$A_X = A \cos(\alpha)$, $A_Y = A \sin(\alpha)$, and $B_X = -B \cos(\beta)$, $B_Y = -B \sin(\beta)$,

Hence, the equilibrium equations of the mid-body region become:

$$\sum F_X : \quad [A\cos(\theta) - B\cos(\theta) + (F_I + F_C)(\cos(\theta) - \cos(\theta)) + W_X] = 0 \tag{8}$$

$$\sum F_Y : \quad [A\sin(\theta) - B\sin(\theta) + (F_I - F_C)(\sin(\theta) + \sin(\theta)) + W_Y] = 0 \tag{9}$$

$$\sum M_Z : \quad [(d_A \times A) + (d_I \times F_I) + (d_C \times F_C) + (d_B \times B) + (d_{PI} \times F_I) + (d_{PC} \times F_C) + (d_W \times W)] = 0 \tag{10}$$

where the standard sign convention for θ and θ must be employed; and taking moments about W:

$$(\sum M_Z)_W = 0: \quad (d_A \times A) = -[(d_I \times F_I) + (d_C \times F_C) + (d_B \times B) + (d_{PI} \times F_I) + (d_{PC} \times F_C) \tag{11}$$

For the caudal region, where $r_C \leq P \leq FL$, and where FL is the total fish length :

$$\sum F_X : \quad [B_X - P_{IX} - P_{CX} - T_X](i) = -[m_C a_X](i) \tag{12}$$

$$\sum F_Y : \quad [B_Y - P_{IY} + P_{CY} - T_Y](j) = [m_C a_Y](j) \tag{13}$$

$$\sum M_Z : \quad [(d_B \times B) + (d_{PI} \times P_I) + (d_{PC} \times P_C) + (d_T \times T)](k) = [(d_G \times m_C a) + I_{CZ}\,\theta_{CZ}](k), \tag{14}$$

Noting that a boundary condition at FL is that the moment is zero; we take moments about T:

$$(\sum M_Z)_T = 0: \quad (d_B \times B) = -(d_{PI} \times P_I) - (d_{PC} \times P_C) + (d_G \times m_C a) + I_{CZ}\,\theta_{CZ}. \tag{15}$$

In order to use equation 15, we must determine the location of the TP defining the ends of the mid-body region (see Fig. 2). Once the locations of the TP's are identified, the linear and angular accelerations may be calculated for both the rostral and caudal portions from specimen measurements and kinematic data analysis; the external reactive forces may then be determined in terms of the muscular forces. Solving equation 15 for B, with further substitution into the mid-body and rostral regions, allows for the determination of the moment, M_{PR} , at any point along the midline of the fish. The flexural rigidity, EI, may then be determined at any section along the fish using the equation:

$$MR = EI,$$

where $M = M_{PR}$, R is the radius of curvature, E is Youngs modulus, and I is the cross-sectional area moment of inertia about which bending occurs.

Materials and Methods

Four specimens of pumpkinseed sunfish (*Lepomis gibbosus*) were collected by seine net from Sunset Lake on the Vassar College campus. The specimens ranged in total length from 10.5cm to 13.30 cm (12.01 ± 0.58 SEM), weighed from 23.37 g to 50.74 g (35.66 ± 5.70 g SEM), and had densities ranging from 0.72 g cc^{-1} to 0.84 g cc^{-1} (0.79 ± 0.02 g cc^{-1} SEM). The four specimens were transferred to a 110L glass holding tank where the water temperature was maintained at approximately 20 ^{O}C. All fish were fed with a daily diet of commercial dry fish pellets; food was withheld on the day of the experiments.

Experimental Protocol

Each specimen was transferred to a 75L glass experimental tank previously filled to a depth of 12.0 cm with water from the holding tank. The fish was allowed to acclimate for at least thirty minutes prior

to testing. A mirror was mounted at a 45° angle directly below the glass bottom of the tank; the set up was back lit by a 500 W high intensity quartz halogen work light (model BD-8U, Bull Dog Power Light). A high-speed video camera (model Ektapro intensified imager and EM 1000 processor, Kodak Motion Systems, Inc.) was positioned 2 m from the mirror and it recorded the ventral view of the fast start event at a capture rate of 1,000 images per second. Fast-start swimming responses were elicited by dropping a cushioned weight into the tank.

Electromyography

Prior to surgery, offset twist bipolar hook electromyography (EMG) electrodes were fabricated from 0.05 mm stainless steel wire (California Fine Wire Co.) according to Loeb and Gans (1986). Each fish was then anesthetized by submerging the individual in a 1:10,000 dose of tricaine (sold as Finquel, Argent Chemical) for approximately eight minutes. From a lateral approach, a 23 gauge hypodermic needle (Becton-Dickinson) was used to percutaneously implant the EMG electrodes into the white (anaerobic or "fast") musculature of the fish. Bilateral implantation of electrodes was achieved at three positions along the length of the fish: just posterior to the gills, mid-length, and peduncle. The EMG wires were taped together and threaded through the dorsal fin to prevent impingement or electrode removal during the experiment (Jayne and Lauder, 1993). Anesthesia was maintained during the surgical procedure by flushing the gills; surgery lasted approximately one hour. The fish was transferred to the experimental tank where it was allowed to recover for at least thirty minutes prior to the commencement of the experiment. EMG signals were amplified (A-M Systems differential AC amplifier) with low and high band pass filter settings of 100 Hz and 10,000 Hz, a 60 Hz notch filter, and a gain setting of 10,000. The EMG signals were recorded using an eight-track digital audio recorder (model ADAT, Alesis Corp.). After five fast-start events were recorded from each specimen, the fish was then euthanized with an overdose of 1:5,000 solution of tricaine. The length, weight, and volume of each specimen was then measured and recorded.

EMG and Kinematic Analysis

EMG signals and kinematic recordings were analyzed off-line. EMG signals from the digital tape were sampled at 6 kHz per channel using an analog-to-digital converter (LabVIEW version 3.0 and NB-MIO-16L board, National Instruments Inc.) and computer (model Macintosh IIfx, Apple Corp.). Times of EMG onset and offset were defined by the appearance of voltage above average baseline noise. The beginning of the fast start was identified by the presence of simultaneous, high-amplitude EMG spikes for all channels (see Fig. 4), a pattern characteristic of Mauthner-cell firing ($\leq$ 0.001 seconds difference between onsets). Beginning at the time of EMG onset, video images, which were synchronized with the EMG signal *via* two common EMG channels recorded on the video, were analyzed frame-by-frame using a genlock to overlay computer and video signals (model TelevEyes, Digital Vision, Inc.). Using an on-screen digitizing grid (NIH Image version 1.51), each image was calibrated using a 10 cm x 10 cm reference grid in each frame of the image. Twenty points were then digitized along each outer edge of the fish, rostral to caudal, for a total of forty points per image. Midlines of 31 points for each image were reconstructed using a custom program that employs weighted splines (Jayne & Lauder, 1993).

For each midline, its set of x-, y-coordinates was fit with a least-squares regression, resulting in a continuous function $y = F(x)$. The first and second derivatives, y' and y'', were then taken to evaluate the radius of curvature, R, along the fish, where:

$$R = \frac{[1 + (y')^2]^{3/2}}{|(y'')|}$$

From these continuous functions defining the midlines, the TP points of the column were determined by

solving the functions simultaneously using Mathematica (version 3, Wolfram, Cambridge, MA).

Calculation of Muscle Force

The force generated by the musculature to initiate the fast-start motion was calculated from data obtained in the literature. Specifically, using values for the mean power output (PO) of 167 W Kg^{-1}, a length-specific contraction velocity (CV) of 13.15 s^{-1} for *Serratus cabrilla*, (Wakeling and Johnston, 1998), and the mean muscle mass per length g $(mm)^{-1}$ (ML) as determined from cross-sectional data, we estimated the maximum force, F_{MAX} , produced by the muscle on the concave side of bending from the following equation:

$$F_{MAX} = (ML \times PO) / CV$$

A function curve for a unit force, F_U , was then generated from the time data to reach half-maximum force and the time from maximum force to half-relaxation — 9.32 ms and 30.49 ms, respectively (Wakeling and Johnston, 1998). This forcing function is represented by the equation:

$$F_U = \begin{cases} (0.0536)t, & \text{for } t \leq 9.32 \text{ ms} \\ (0.103)t - 0.46 & \text{for } 9.32 \text{ ms} < t \leq 14.18 \text{ ms} \\ 1 & \text{for } t > 14.18 \text{ ms.} \end{cases}$$

The estimated force generated on the ipsilateral (concave) side of bending, F_I , at a given time within the stage 1 fast start cycle is obtained by multiplying F_{MAX} by F_U . The force produced by the contralateral (*i.e.*, that on the convex side of the bending body) muscle, F_C , at a given time was taken as F_I multiplied by the ratio of the EMG peak heights (contralateral divided by ipsilateral) at stage 1 onset. F_I and F_C are the magnitudes of the forces transmitted along the length of their muscles and are distributed across the muscles' cross-sectional area. These forces, however, were treated as point loads, acting through the effective center of the muscle, whose resultant vector was taken as the tangent to the curve describing the position of the center with respect to the midline.

Cross-sectional Data

Four specimens were euthanized with an overdose of tricaine. Each specimen was then tagged and placed into a solution of ten percent formaldehyde for forty-eight hours after which each was rinsed with water, blotted dry, and frozen at -40° C for another 48 hours. The specimens were then removed from the freezer and reweighed using an electronic balance; the peduncle, fork, and total lengths were measured. The total volume of each specimen was then determined by water displacement, and the total density was calculated. Each specimen was then transected at various locations along the length of the fish; each section was then weighed, allowing for the generation of a mass distribution curve. After weighing, the cross-section was digitally imaged and digitized (NIH Image v 1.51). The digitized points were then curve-fitted with a polynomial function, y = F(z), such that the area and its center from the vertical septum were calculated for anatomical entities (*i.e.*, muscle, gut, etc.), according to the following:

$$\text{Area} = \int_A dA, \text{ where } dA = y(dz),$$

and

$$\text{y-center} = \frac{\int_A (y/2)dA}{\int_A dA}.$$

For a given cross-section the effective moment arm of the muscle was determined by:

$$\sum (y\_center)_i \, (area)_i \, / \sum (area)_n ,$$

where i is an anatomic entity, and n is the total number of entities. The muscle center was then defined as a function of fish length.

Calculations of Rostral and Caudal Centers of Mass

Once the location of the rostral and caudal TP's were determined, the mass of both portions was calculated from the mass distribution curve generated from the sectioned specimens using the following:

$$\text{Mass} = \int_m dM, \text{ where } dM = \rho dL, \text{ and } \rho = \frac{dM}{dL} = \text{linear mass density}$$

The position of the rostral mass center along the midline of the fish was calculated for each frame by:

$$\text{Mass center} = \frac{\int_m (L/2)\rho dM}{\int_m \rho dM},$$

The center of mass for the caudal region was taken as acting halfway between the caudal TP and the end of the caudal fin, since we modeled the caudal fin as a 2-D plate with a constant mass distribution. Thus, the mass moment of inertia about the z-axis was taken as $(1/12)mL^2$ where L is the plate length.

Calculating Linear and Angular Accelerations

The locations of the mass centers were transformed into their respective x-,y-coordinates and each was defined as a function of time. The vector between the rostral center of mass and the TP separating the rostral body was determined; the angle defining the vector was determined as a function of time. Both the linear and angular accelerations were defined by taking their second derivative from their respective equations. A similar analysis was performed for the caudal mass center.

Results

A fast-starting sunfish reconfigures its body from straight to maximal curvature in 35 ms during stage 1 (Figs. 1 & 3). This motion is the result of simultaneous muscle activity on and along both sides of the body (Fig. 4). Since only the middle portion of the body reconfigures (Fig. 3), the whole-body can be

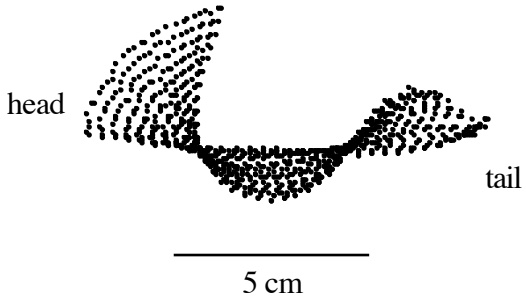

Figure 3. Reconstructed midlines, overlaid, of a fast-starting sunfish (12.0 cm total length; 32.3 g total mass). The portion of the fish behaving, at any time, as a beam was defined as that part between the nodes. Note that while the position of the nodes remains relatively stationary, the sunfish's body translates through those nodes as reconfiguration proceeds from a straight to a tightly curved shape (see also Fig. 1); thus, the portion of the fish behaving as a beam increases as stage 1 progresses.

modeled as a beam-column hybrid (Fig. 2). The parts of the body that act as an inflexible beams, as defined by rotation without lateral deflection, include the head and the anterior region of the body. The part of the body that acts as a column, defined by deflection without rotation, includes most of the body containing lateral musculature, the region from the anterior beam to the caudal peduncle, 0.33 to 0.74 L (Fig. 5A). Muscle activated on both sides of the body initially generates a standing wave of bending moment that is followed by a traveling wave of moment (Fig. 5A). Maximal bending moments are inversely correlated with axial position (Fig. 5B). These moments combine with the changing body curvature to produce effective (sum of passive and muscular components) flexural stiffnesses that peak early in the cycle and differ along the body (Fig. 5C).

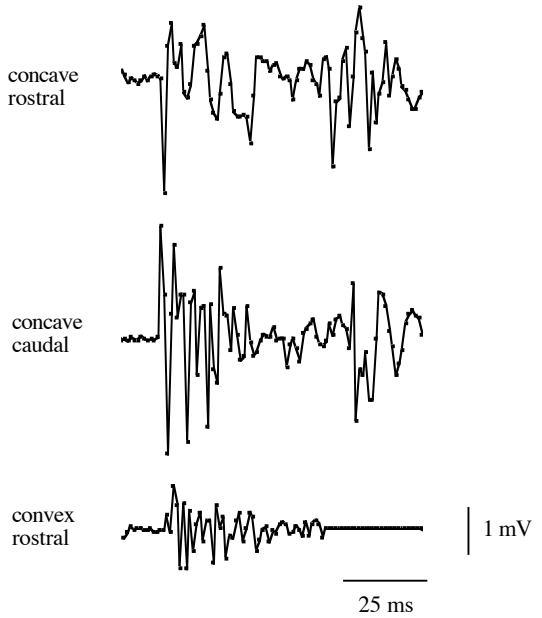

Figure 4. Electrical activity patterns of locomotor muscle of a pumpkinseed sunfish (same trial as that in Fig. 3) during a fast start, as measured using electromyography. "Concave" refers to the side towards which the fish bends during stage 1; "convex" refers to the opposite side. Simultaneous, high-amplitude spikes initiating electrical onset indicate Mauthner-cell activation (first two traces). Signal on opposite side (bottom trace) indicates nearly-simultaneous activation of this antagonistic muscle. Traces sampled at 2 kHz from 40 kHz digital tape.

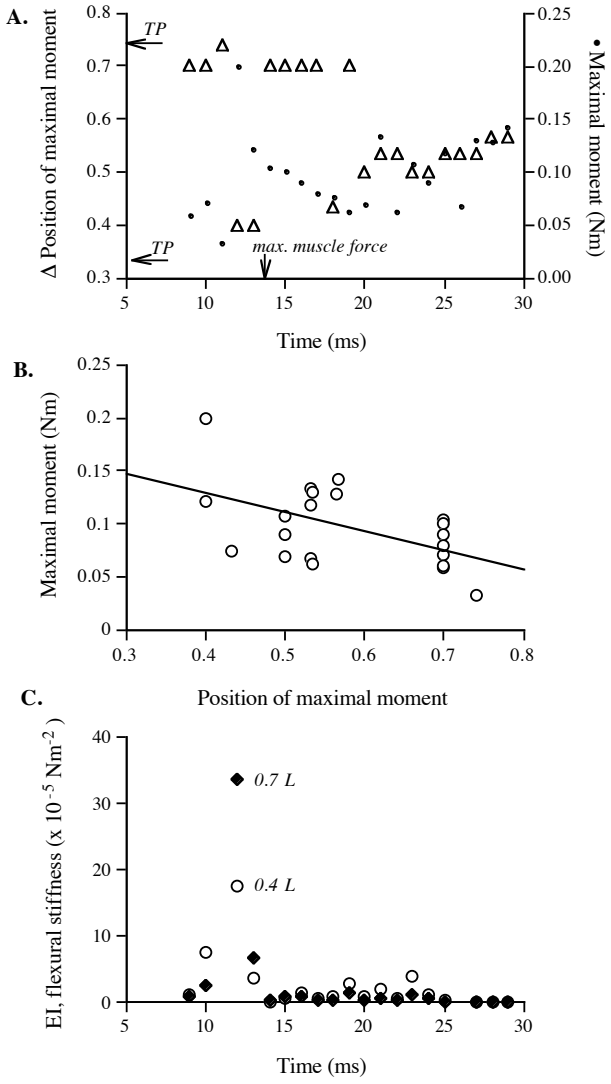

Figure 5. Fast-start mechanics of a pumpkinseed sunfish (same individual and trial as that in Figs. 3 & 4) during stage 1 as predicted by the beam-column model. **A**. Bending moments. Within the column section of the body (between transition points, labeled "TP", from 0.33 to 0.74 L), the axial position of the maximal moment (open triangles) remains almost stationary at 0.7 L until 18 ms, when the maximal moment travels rearward from 0.43 L to 0.57 L. The magnitude of the moments (filled circles) varies with time, peaking at 12 ms, with a magnitude of 0.20 Nm just before maximal muscle force is reached. **B**. Position and magnitude of the bending moments are negatively correlated ($r^2 = 0.24$, $p < 0.05$), with magnitude of the bending moments decreasing posteriorly. **C.** Effective flexural stiffness, EI, of the body varies with time and axial position. At 12 ms into the fast start, EI peaks at 0.4 and 0.7 L, with the posterior EI achieving a magnitude nearly twice that of the anterior position. At both sites, EI decreases dramatically. Please note that the effective flexural stiffness is a function of the combined bilateral muscle activity, the passive material and structural properties of the body, and the external loads.

Discussion

When modeled as a column undergoing high-amplitude deflections caused by internal, asymmetric axial loads, the body of a fast-starting sunfish produces first a standing wave of maximal bending moment at 0.7 L and then a traveling wave of maximal bending moments that moves from 0.42 to 0.57 L (Fig. 5). While a combined standing-traveling wave of bending moment has been predicted from theory in steadily swimming saithe, *Pollachius virens* (Cheng & Blickhan, 1994), the relative axial placement was reversed. Cheng & Blickhan (1994) hypothesized that the anterior region, with its standing moment wave, was the motive source responsible for initiating the traveling bending (*i.e.,* kinematic or propulsive) wave, while the posterior region, with its traveling wave of bending moment, propagated the traveling bending wave.

With this in mind, our results suggest that fast-starts, relative to steady swimming, require a reversal of motive and propagating regions of the body. This interpretation is consistent with the maximal flexural stiffnesses predicted by the model; anterior and posterior EI peak simultaneously at 12 ms, when the standing moment wave is present (Fig. 5A & C; note that the placement of the moment wave is , at 12 ms, at 0.4 L not 0.7 L — nearly identical moment values throughout this region of the body at this time cause the appearance of a standing wave jumping from posterior to anterior position). This large increase

in stiffness is the consequence of simultaneous (though unequal) muscle activity on both sides of the body (see Fig. 4), and the active muscle on the convex side of the body resists the change in length caused by the muscle on the concave side of the body. Since the body is stiff when the standing moment wave is present, motive moments from the posterior region are rapidly transmitted to the anterior regions. The rapid decline in flexural stiffness that follows (Fig. 5C) permits the transmitted moments to work to bend the body into a tight C-shape (Fig. 1 & 3) in preparation for the thrust-producing stage 2.

For engineers interested in designing adaptable structures capable of rapid reconfigurations, the body of a fast-starting fish offers several insights. First, transient alterations in the flexural stiffness of the structure permit the structure to act, over the course of a particular continuous action, as both a motor and transmission system. Second, actively antagonist forces generate a situation in which the mechanical behavior of the structure (EI, motion of the moment wave, body shape) can be rapidly altered.

Acknowledgements

This work was funded by the Office of Naval Research (ONR #N-00014-97-1-0292 to JHL & RGR). We wish to thank, for their helpful suggestions, Robert Suter and Hayden-William Courtland.

References

Alhorn, B., Chapman, S., Stafford, R, Blake, R.W. & Harper, D.G. 1997. Experimental simulaton of the thurst phases of fast-start swimming of fish. *J. exp. Biol*. 200: 2301-2312.

Beamish, F.W.H. 1978. Swimming capacity. In. Fish Physiology, vol. VII, ed. W.S. Hoar and D.J. Randall, pp. 101-187. Academy Press, New York.

Beddow, T.A., van Leeuwen, J.L. & Johson, IA. 1995. Swimming kinematics of fast starts are altered by temperature acclimation in the marine fish *Myoxocephalus scorpius*. *J. exp. Biol*. 198:203-208.

Beer, F.P., and Johnston, E.R., Jr. 1977. VECTOR MECHANICS FOR ENGINEERS: DYNAMICS, 3rd edition, McGraw-Hill BooK Co., New York.

Cheng, J. & Blickman, R. 1994. Bending moment distribution along swimmimg fish. *J. Theor. Biol.* 168:337-348.

Cheng, J.-Y., Pedley, T.J., and Altringham, J.D. 1998. A continuous dynamic beam model for swimming fish. *Proc. R. Soc. Lond*. ?:981-997.

Covell, J.W., Smith, S., Harper, D.G., and Blake, R.W. 1991. Skeletal muscle deformation in the lateral muscle of the intact rainbow trout *Oncorhynchus mykiss* during fast start maneuvers. *J. Exp. Biol*. 156:453-466.

Domenici, P. & Batty, R.S. 1994. Escape manoeuvres of schooling *C. harengus*. *J. Fish Biol*. 45 (Suppl.), 97-110.

Domenici, P. and Blake, R.W. 1991. The kinematic and performance of the escape response in the anglefish (*Pterophyllum eimekei*). *J. Exp. Biol*.. 156:187-205.

Domenici, P. and Blake, R.W. 1993. Escape trajectories in anglefish (*Pterophyllum eimekei*). *J. Exp. Biol*.. 177:253-272.

Domenici, P. and Blake, R.W. 1997. Review: the kinematics and performance of fish fast-start swimming. *J. Exp. Biol*. 200:1165-1178.

Eaton, R.C., Bombardieri, R.A., and Meyer, O.H. 1977. The Mauthner-inititated startle response in teleost fish. *J. exp. Biol*. 66:65-81.

Eaton, R.C., Lavender, W.A. and Wieland, C.M. 1981. Identification of Mauthner-initiated response patterns in goldfish: evidence from simultaneous cinematography and electrophysiology. *J. Comp. Physiol*. 144:521-531.

Fernald, R.D. 1975. Fast body turns in a cichlid fish. *Nature* 258:228-229.

Frith, H.R. and Blake, R.W. 1991. Mechanics of the startle response in the northern pike, *Esox lucius*. *Can. J. Zool*. 69:2831-2839.

Frith, H.R. and Blake, R.W. 1995. The mechanical power output and the hydromechanical efficiency of northern pike (*Esox lucius*) fast starts. *J. exp. Biol*. 198:1863-1873.

Gamperl, A.K., Schnurr, D.L. and Stevens, E.D. 1991. Effect of a sprint-training protocol on acceleration performance in rainbow trout (*salmo gairdneri*). *Can. J. Zool*. 69:578-582.

Harper, D.G. and Blake, R.W. 1990. Fast-start performance of rainbow trout *Salmo gairneri* and northern pike *Esox lucius*. *J. Exp. Biol*. 198:1863-1873.

Hess, F. and Videler, J.J. 1984. Fast continuous swimming of swimming saithe (Pollachius virens): a dynamic analysis of bending moments and muscle power. *J. Exp. Biol*. 109:229-251.

Hibbeler, R.C. 1978. ENGINEERING MECHANICS: STATICS, 2nd ed., Macmillan Pub. Co., Inc., New York.

Jayne, B.C. and Lauder, G.V. 1993. Red and white muscle activity and kinematics of the escape response of the bluegill sunfish during swimming. *J. Comp. Physiol*. A 173:495-508.

Johnson, T.P., Cullum, A.J., and Bennett, A.F. 1993. The thermal dependence of C-start performance in fish: physiological versus biophysical effects. *Am. Zool*. 33:65A.

Johnson, T.P., Cullum, A.J., and Bennett, A.F. 1998. Partitioning the effects of temperature and kinematic viscosity on the C-start performance of adult fishes. *J. exp. Biol*. 201:2045-2051.

Kasapi, M.A., Domenici, P., Blake, R.W. and Harper, D.G. 1993. The kinematics and performance of the escape response in the knifefish *Xenomystus nigri*. *Can. J. Zool*. 71:189-195.

Loeb, G.E. and Gans, C. 1986. Design and construction of electrodes. In. Electromyography for Experimentalists. The University of Chicago Press, Chicago, Ill. pp. 109-122.

Lighthill, M.J. 1971. Large-amplitude elongated-body theory of fish locomation. *Proc.R.Soc.Lond*.B 179:125-138.

Nissanov, J. & Eaton, R. 1989. Reticulospinal control of rapid escape turning maneuvers in fishes. *Am. Zool*. 29:103-121.

Webb, P.W. 1976. The effect of size on the fast-start performance of rainbow trout *Salmo gairdneri* and a consideration of piscivorous predator-prey interaction. *J. exp. Biol*. 65:157-177.

Webb, P.W. 1977. Effects of median fin amputation on fast-start performance of rainbow trout (*Salmo gairdneri)*. *J. exp. Biol*. 68:123-135.

Webb, P.W. 1978. Fast start performance and body form in seven species of teleost fish. *J. exp. Biol*. 74:211-226.

Webb, P.W. and Blake, R.W. 1985. Swimming. In. Functional Vertebrate Morphology, eds. M. Hildebrand, D.M. Bramble, K.F. Liem, and D.B. Wake. pp. 110-128. The Belknap Press of Harvard University, Cambridge, MA.

Weihs, D. 1973. The mechanism of rapid starting of slender fish. *Biorheology*. 10:343-350.